• Basic Research •

4D label-free proteomic analysis of vitreous from patients with rhegmatogenous retinal detachment

Qiu-Yi Huo[1], Meng-Chao Zhu[1], Wen-Chao Yang[2], Yi-Peng Wang[2], Song Chen[3]

[1]Wenzhou Medical University, Wenzhou 325027, Zhejiang Province, China
[2]Anyang Eye Hospital, Anyang 455000, Henan Province, China
[3]Tianjin Eye Hospital, Tianjin Eye Institute, Tianjin Key Lab of Ophthalmology and Visual Science, Nankai University Affiliated Eye Hospital, Tianjin 300020, China
Co-first authors: Qiu-Yi Huo and Meng-Chao Zhu
Correspondence to: Song Chen. Tianjin Eye Hospital, Tianjin Eye Institute, Tianjin Key Lab of Ophthalmology and Visual Science, Nankai University Affiliated Eye Hospital, Tianjin 300020, China. chensong9999@126.com; Yi-Peng Wang. Anyang Eye Hospital, Anyang 455000, Henan Province, China. dearyipeng@163.com
Received: 2022-12-14 Accepted: 2023-03-06

Abstract

● **AIM:** To identify metabolites, proteins, and related pathways involved in the etiology of rhegmatogenous retinal detachment (RRD) for use as biomarkers in diagnosing and treating RRD.

● **METHODS:** Vitreous specimens were collected and liquid chromatography-tandem mass spectrometry analysis was performed using the four-dimensional label-free technique. Statistically significant differentially expressed proteins, gene ontology (GO) terms, Kyoto Encyclopedia of Genes and Genomes (KEGG) pathway representations, and protein interactions were analyzed.

● **RESULTS:** Nine specimens were subjected to proteomic analysis. In total, 161 proteins were identified as differentially expressed proteins (DEPs), including 53 upregulated proteins and 108 downregulated proteins. GO functional analysis revealed that some DEPs were enriched in neuron-related terms and membrane protein terms. Moreover, KEGG analysis indicated that the cell adhesion molecule metabolic pathway was associated with the greatest number of DEPs. Finally, the evaluation of protein-protein interaction network revealed that DEPs were clustered in neuronal adhesion, apoptosis, inflammation and immune responses, correct protein folding, and glycolysis.

● **CONCLUSION:** Proteomic profiling is useful for the exploration of molecular mechanisms that underlie RRD. This study reveals increased expression levels of proteins related to heat shock protein content, glycolysis, and inflammatory responses in RRD. Knowledge regarding biomarkers of RRD pathogenesis may help to prevent the occurrence of RRD in the future.

● **KEYWORDS:** vitreous; rhegmatogenous retinal detachment; proteome; 4D label-free
DOI:10.18240/ijo.2023.04.05

Citation: Huo QY, Zhu MC, Yang WC, Wang YP, Chen S. 4D label-free proteomic analysis of vitreous from patients with rhegmatogenous retinal detachment. *Int J Ophthalmol* 2023;16(4):523-531

INTRODUCTION

Rhegmatogenous retinal detachment (RRD), an ophthalmic emergency with an annual incidence of 1:10 000[1], carries a risk of permanent visual impairment if left untreated. RRD results from retinal tears or holes caused by vitreal traction on the retina[2]. Vitreous fluid drains into the subretinal space, separating the sensory retina from the underlying retina. Hypotension occurs in eyes with RRD[3-4]; surgery is the only effective therapeutic approach. RRD is usually repaired via scleral buckle, pars plana vitrectomy, or a combination of the two procedures[5]. Surgical techniques and instruments developed over the past few decades have achieved primary reattachment rates of approximately 95%[6]. Separation of the sensory retina from the retinal pigment epithelium leads to irreversible photoreceptor loss, with pathogenic processes that include apoptosis, necrosis, and oxidative stress[7-9]. Although multiple factors are associated with the risk of RRD, its pathogenesis has not been fully elucidated.

Proteomic analysis enables extensive investigation of differently expressed proteins (DEPs). Proteomic technologies can accurately quantify and identify the vast majority of proteins expressed in the genome[10]. Commonly used quantitative proteomic techniques include isotope tagging for relative and absolute quantification (iTRAQ), tandem mass tags, and label-free quantification techniques. Recently,

a 4D label-free technique has been used for proteomic analysis because of its high sensitivity and bioinformatics advantages[11], particularly for valuable or limited samples. This new proteomic approach can detect many proteins with low abundance[12]. Additionally, label-free proteomic analysis is useful for biomarker exploration because it can identify a wide range of associated proteins[13].

This study was conducted to compare proteomic profiles of vitreous samples from patients with RRD and patients with epiretinal membrane (EM), including the underlying molecular pathogenesis, using the 4D label-free technique and a bioinformatics analysis approach. In contrast to many other blinding retinal diseases, there is a possibility for avoidance or prevention of RRD if the underlying molecular biological mechanisms are elucidated.

SUBJECTS AND METHODS

Ethical Approval The present study was performed in accordance with the Declaration of Helsinki, and the study protocol was approved by the Medical Ethics Committee of Anyang Eye Hospital (No.AYLS-2022-01). Patients provided written informed consent to participate in the study.

Clinical Samples Vitreous samples from patients with RRD and patients with EM were collected from Anyang Eye Hospital. Exclusion criteria included diabetes, hypertension, cardiovascular diseases, and other systemic diseases. Vitreous samples were collected during vitrectomy and rapidly stored at -80℃. Five RRD samples and four EM samples were subjected to 4D label-free mass spectrometry.

Protein Extraction and Trypsin Digestion Samples were extracted by the SDT [4% (w/v) sodium dodecyl sulfate, 100 mmol/L Tris/HCl pH 7.6, 1 mmol/L dithiothreitol] lysis method; protein concentrations were quantified using the bicinchoninic acid method. The 200 μg of protein was collected from each sample, then subjected to filter-aided proteome preparation *via* trypsin enzymolysis. C18 cartridges were used to desalt the resulting peptides. Subsequently, peptides were lyophilized and redissolved in 40 μL of 0.1% formic acid solution. Finally, peptides were quantified by reading the absorbance at 280 nm.

Liquid Chromatography-Tandem Mass Spectrometry Analysis Each sample was separated using the Easy nLC high-performance liquid chromatography liquid phase system with a nanoliter flow rate. Buffer A was 0.1% formic acid aqueous solution and buffer B was 0.1% formic acid acetonitrile aqueous solution. The chromatographic column was equilibrated with 95% liquid A; each sample was loaded from the autosampler into the loading column (Thermo Scientific Acclaim PepMap100), then passed through the analytical column (Thermo Scientific EASY column) at a flow rate of 300 nL/min. After chromatographic separation, samples were analyzed by mass spectrometry using a timsTOF Pro mass spectrometer in positive ion mode. The ion source voltage was set to 1.5 kV; MS and MS/MS analyses were conducted using the time-of-flight method. The mass spectrometer scan range was set to 100-1700 m/z. Data acquisition was conducted using the parallel accumulation serial fragmentation (PASEF) mode; 10-fold PASEF mode acquisition of mother ions was performed after first-level mass spectrum acquisition, using a cycle window time of 1.17s. For secondary spectra with charge numbers of 0-5, the dynamic exclusion times of MS/MS scans were set to 24s to avoid repeated analyses of parent ions.

Database Search and Bioinformatics Analysis The resulting Liquid Chromatography-Tandem Mass Spectrometry (LC-MS/MS) data were quantitatively analyzed using MaxQuant software (version number 1.6.14). First, quantitative data regarding the target protein set were normalized to an interval of (-1,1). Then, the Complexheatmap R package (R Version 3.4) was used for simultaneous classification of samples and protein expression levels, and a hierarchical clustering heat map was generated. InterProScan software was used for integrated scanning of the InterPro database to achieve functional characterization of each protein sequence; this scanning approach provided domain annotation information regarding the target protein sequence in the Pfam database. Blast2GO and KAAS [Kyoto Encyclopedia of Genes and Genomes (KEGG) Automatic Annotation Server] software were used to perform gene ontology (GO) annotation and KEGG pathway annotation, respectively, of the target protein collection. Fisher's exact test was used to perform GO annotation, KEGG pathway annotation, or domain annotation enrichment analysis of the target protein set. Information from the STRING (http://string-db.org/) database was used to identify direct and indirect interactions between target proteins. Cytoscape software (version number: 3.2.1) was used to generate and analyze the interaction network.

Statistical Analysis All statistical analyses were conducted using SPSS26 software. Data are expressed as means±standard deviations. Student's *t*-test was used to analyze differences between two groups; the threshold of $P<0.05$ was considered statistically significant. Because this was an exploratory study, no sample size calculations were performed.

RESULTS

General Information In total, nine patients were included in this study: five in the RRD group and four in the EM group. The number, age, and sex distribution of each patient group are shown in Table 1, along with the protein concentration and total number in each group.

Identification of Significantly Differentially Expressed Proteins Through strict quality control, 60 146 matched

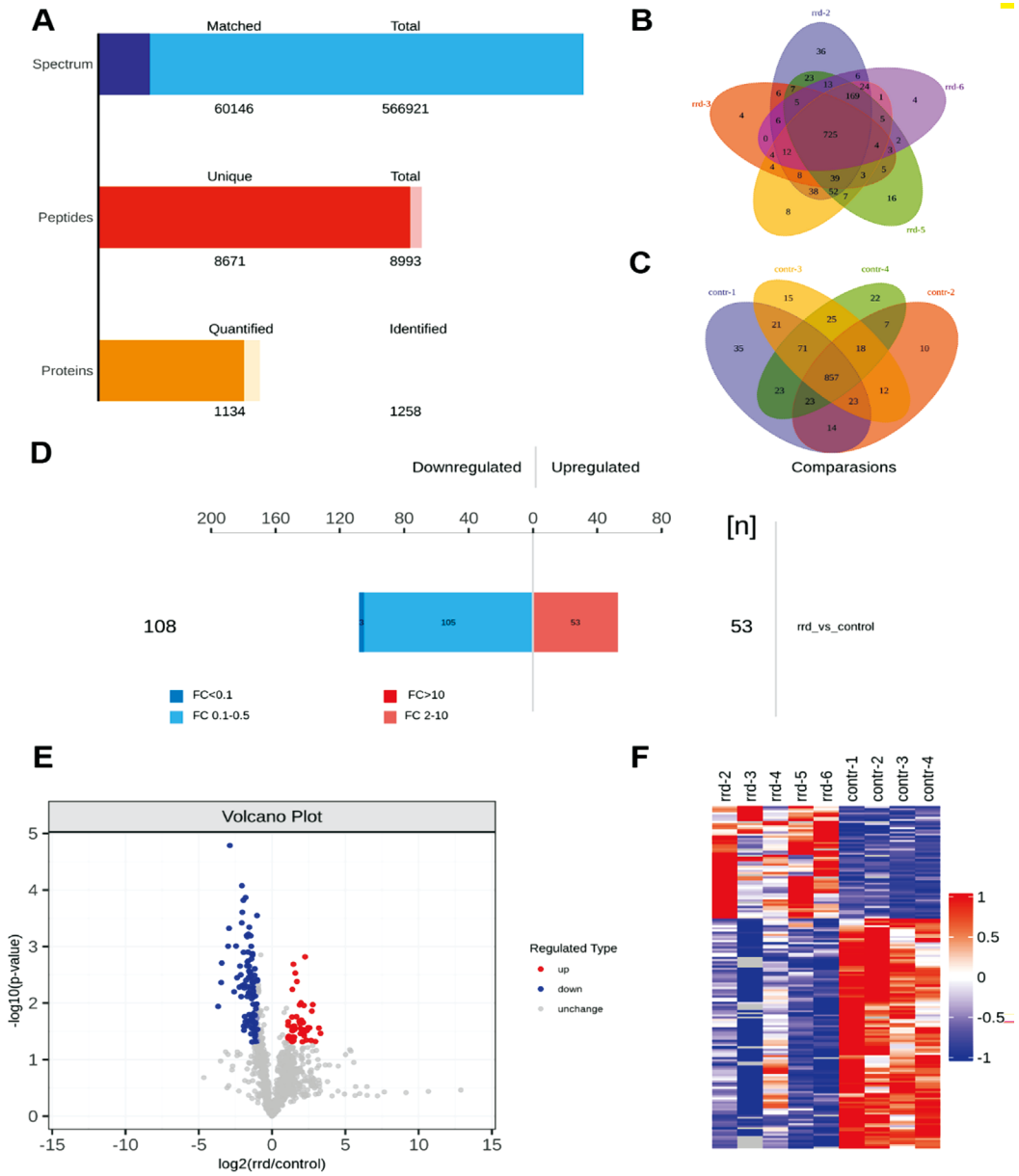

Figure 1 Quantitative proteome analysis A: Bar chart of identification and quantification. B: Quantitative Venn diagram of proteins shared among RRD samples. C: Quantitative Venn diagram of proteins shared among control (EM) samples. D: Histogram of quantitative differences in protein expression. E: Volcano plot of significant DEPs. Upregulated and downregulated DEPs are shown in red and blue. F: Cluster analysis chart depicting significant DEPs. RRD: Rhegmatogenous retinal detachment; EM: Epiretinal membrane; DEPs: Differently expressed proteins.

spectra, 8993 peptides, 1258 identified proteins, and 1134 quantifiable proteins were obtained (Figure 1A). In the RRD group, 725 proteins overlapped; in the control group, 857 proteins overlapped (Figure 1B, 1C). In total, 161 proteins exhibited >2-fold changes in expression (upregulation >2-fold or downregulation <0.50-fold) and *P*-values <0.05 (according to *t*-test analysis) were identified as DEPs, including 53 upregulated proteins and 108 downregulated proteins (Figure 1D, 1E). Hierarchical clustering revealed distinct partitioning of DEPs into distinct clusters that represented RRD and EM groups (Figure 1F).

Gene Ontology Function Analysis GO functional annotation indicated that DEPs were enriched in 54 GO terms (Figure 2A), including 26 biological processes, 16 cellular components, and 12 molecular functions. In terms of biological processes, "cellular process" contained 185 proteins,

Table 1 Clinical characteristics of patients with RRD and patients with EM

Ophthalmic disease	RRD	Control (EM)
No. of patients	5	4
Age (mean±SD)	56±12.7	69.75±7.18
Sex (male/female)	2/3	1/3
Protein concentration (μg/μL±SD)	2.39±1.11	3.25±1.01
Protein groups	1033.6±129.5	1029.75±45.18

RRD: Rhegmatogenous retinal detachment; EM: Epiretinal membrane; SD: Standard deviation. Protein groups: Total number of proteins.

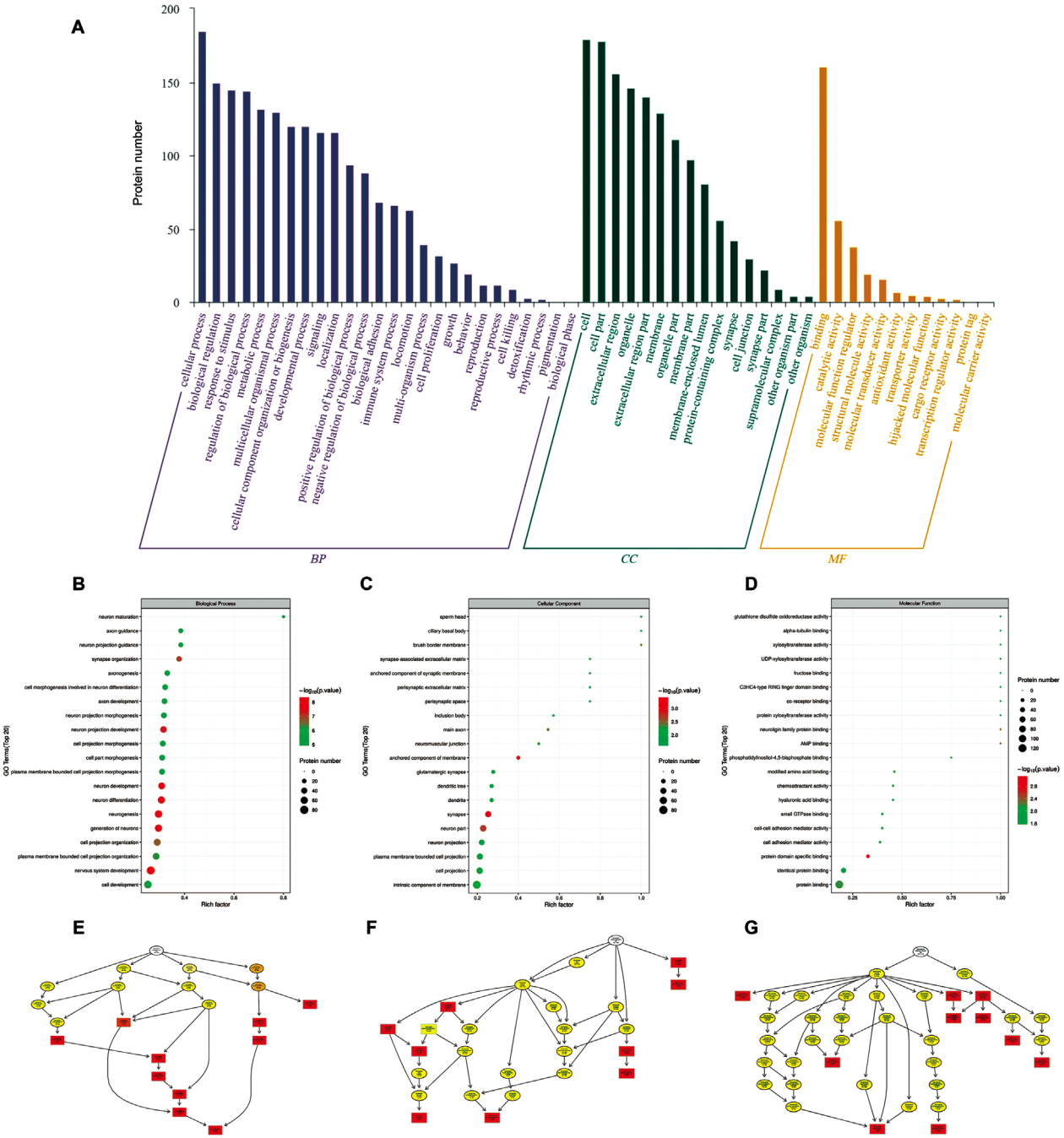

Figure 2 GO classification analysis A: GO classification analysis (RRD *vs* control); each bar represents number of DEPs. B-D: GO function enrichment bubble chart (biological process, BP)/(cellular component, CC)/(molecular function, MF). Top 20 significantly enriched GO terms; dot size represents number of DEPs. E-G: Directed acyclic graphs of the three main classifications (BP)/(CC)/(MF). The main node of each directed acyclic graph represents the top 10 terms with the highest degrees of enrichment, where a darker color indicates a higher degree of enrichment. RRD: Rhegmatogenous retinal detachment; DEPs: Differently expressed proteins.

followed by "biological regulation" (150 proteins), "response to stimulus process" (145 proteins), "regulation of biological process" (144 proteins), "metabolic process" (132 proteins), and "multicellular organismal process" (130 proteins). In terms of cellular processes, "cell process" contained 179 proteins, followed by "cell part" (178 proteins), "extracellular region process" (156 proteins), "organelle" (146 proteins), and "extracellular region part" (140 proteins). In terms of molecular functions, "binding" contained 161 proteins, followed by "catalytic activity" (56 proteins), "molecular function regulator" (38 proteins), "structural molecule activity" (19 proteins), and "molecular transducer activity" (16 proteins). Some upregulated DEPs were enriched in terms related to neurons, including "neuron differentiation," "neurogenesis," "neuron development" and "neuron projection development" (Figure 2B). Furthermore, DEPs were enriched in the terms "synapse", "anchored component of membrane", "intrinsic component of membrane" (Figure

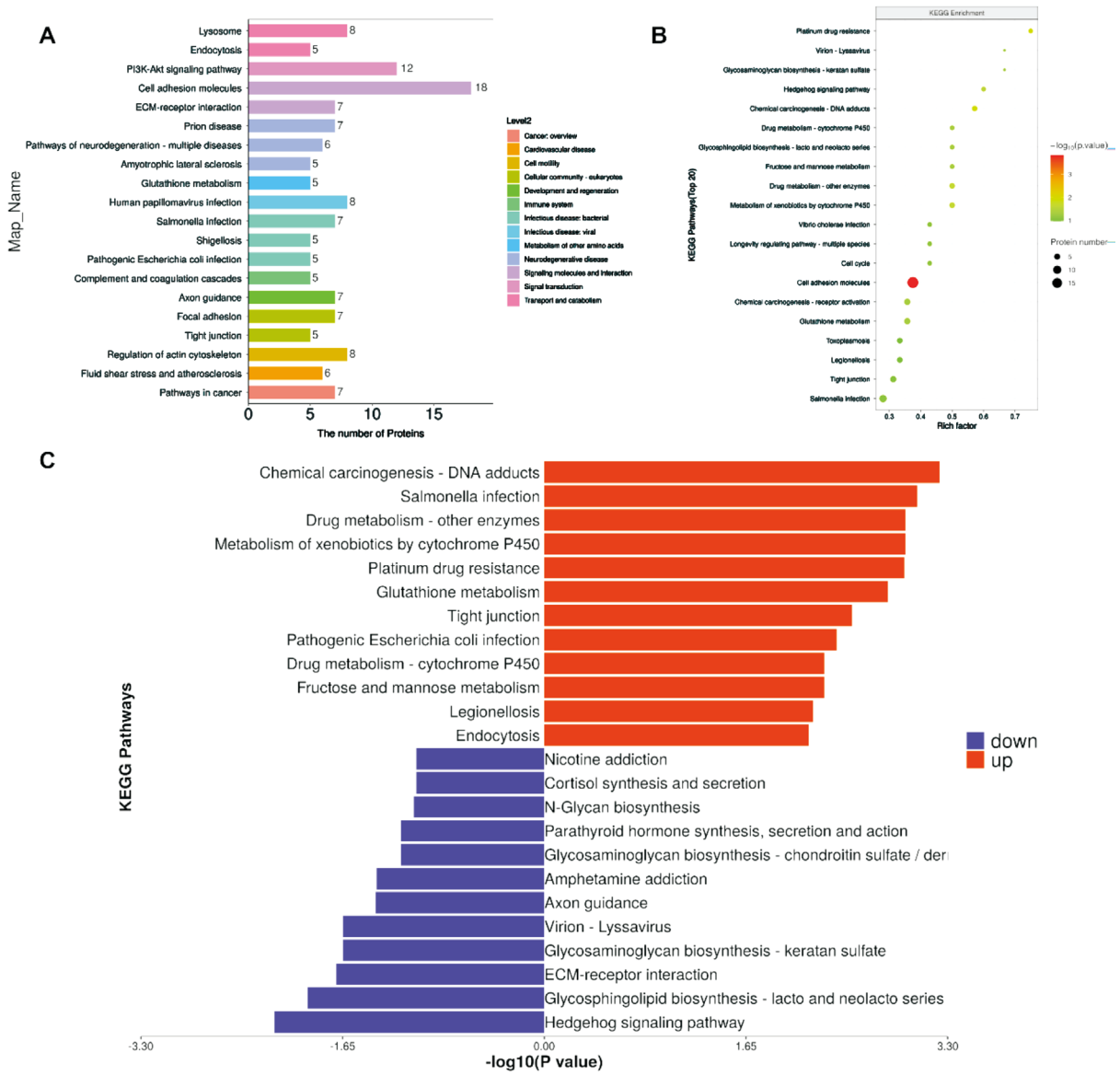

Figure 3 Kyoto Encyclopedia of Genes and Genomes (KEGG) pathway enrichment analysis A: KEGG pathway annotation and attribute histogram of DEPs; different colors represent the seven branches of the KEGG metabolic pathway. B: KEGG pathway enrichment bubble plot. C: Butterfly diagram of up and down regulated DEPs. DEPs: Differently expressed proteins.

2C), and "protein domain specific binding" (Figure 2D). GO directed acyclic graphs were constructed (Figure 2E-2G). Significantly enriched proteins were consistent among the bubble plots.

Kyoto Encyclopedia of Genes and Genomes Functional Annotation and Pathway Enrichment Analysis For further physiological characterization of vitreous samples from patients with RRD and patients with EM, we conducted KEGG pathway enrichment analysis to identify the main biochemical metabolic pathways involving the differential metabolites. In total, 143 differential metabolites were enriched in 20 metabolic pathways (Figure 3A). The cell adhesion molecule metabolism pathway was associated with the largest number of differential metabolites. KEGG pathway analysis revealed that the significantly enriched pathway associated with RRD was the "cell adhesion molecule pathway" (Figures 3B, 4). DEPs in this metabolic pathway were mainly concentrated in the neural system; proteins related to neuronal synapses, growth cones, and axons were all significantly downregulated. In other systems, proteins related to epithelial tight junctions were also downregulated. Cadherins were upregulated, whereas nectins were downregulated. KEGG pathway enrichment analysis of up- and downregulated DEPs (Figure 3C) revealed that upregulated DEPs were mainly enriched in chemical carcinogenesis-DNA adducts, *Salmonella* infection, metabolism of xenobiotics by cytochrome P450, drug metabolism-other enzymes, platinum drug resistance, and glutathione metabolism. Furthermore, downregulated DEPs were mainly enriched in the Hedgehog signaling pathway, glycosphingolipid biosynthesis-lacto and neolacto series, extracellular matrix-receptor interaction, glycosaminoglycan biosynthesis-keratan sulfate, and virion-lyssavirus.

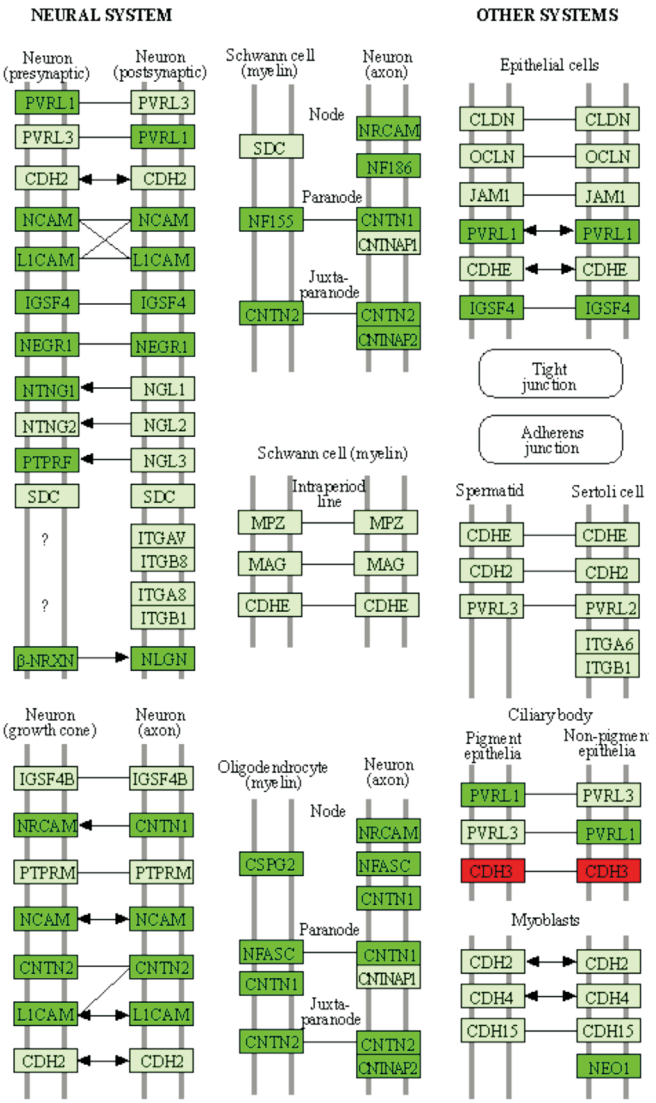

Figure 4 Cell adhesion molecules pathway diagram (has04514).

Protein-Protein Interaction Network Using the STRING online database and Cytoscape software, we established a Protein-protein interaction network of DEPs, comprising 176 nodes and 1434 edges, which included 73 upregulated and 101 downregulated DEPs (Figure 5A). Compared with the control group, DEPs upregulated in the RRD group were mainly enriched in pathways related to cell differentiation, migration and apoptosis, correct protein folding, actin network synthesis, neurite formation, neutrophil chemotaxis adhesion, allergic response, and glycolysis. DEPs downregulated in the RRD group were enriched in pathways related to cell-cell interactions, recognition and adhesion, regulation of neuronal adhesion and axon outgrowth, heparan sulfate and chondroitin sulfate proteoglycan formation, endothelial cell proliferation, migration, and tube formation.

Protein-protein interaction module analysis was implemented using MCODE plugins in Cytoscape; eight significant clusters were identified throughout the network (Figure 5B). The top five clusters with high scores were selected for display: cluster 1 contained 48 nodes, cluster 2 contained 47 nodes, cluster 3 contained 40 nodes, cluster 4 contained 12 nodes and 20 edges, and cluster 5 contained nine nodes and 10 edges. Subsequently, corresponding GO term enrichment analysis was performed using BiNGO plugins in Cytoscape. Genes in cluster 1 were significantly enriched in cell apoptosis, monocyte-macrophage system, acute inflammatory response, allergen sensitization response, and integrin signaling regulation. Moreover, genes in cluster 2 were mainly enriched in cell-cell interactions, cell recognition, cell adhesion, neurite outgrowth of both axons and dendrites, and neuronal circuit formation. Genes in cluster 3 were enriched in a wide variety of cellular processes, including specific target protein maturation, correct folding, intracellular oxidative stress countermeasures, glycolysis and gluconeogenesis, and actin network synthesis. Genes in cluster 4 were enriched in heparan sulfate formation and chondroitin sulfate proteoglycan formation. Finally, genes in cluster 5 were primarily enriched in interactions between cells and the extracellular matrix.

DISCUSSION

RRD is a clinical ophthalmic emergency. Retinal cells, photoreceptors, and retinal pigment epithelium are exposed to liquefied vitreous, thus preventing the entry of oxygen and nutrients into the choroidal vasculature[14-15]. Prompt surgery is often required to prevent further detachment and to restore sensory function. Here, we used 4D label-free technology-based proteomic quantitative analysis to analyze vitreous samples from five patients with RRD and four patients with EM; we sought to identify biomarkers associated with RRD pathogenesis.

Our results demonstrated that the cell adhesion molecule metabolic pathway was associated with the largest number of differential metabolites. Proteins related to epithelial tight junctions were downregulated; cadherins were upregulated, and connexins were downregulated. Furthermore, proteins related to neuronal adhesion, neurite formation, and axonogenesis were downregulated in RRD. Proteins related to the reorganization of cell adhesion molecules and apoptosis were upregulated in RRD[16]. Other studies have shown that the proteins neurexin, selectin, and neuronal cell adhesion molecule were significantly downregulated in patients with RRD, compared with controls[17]. After the onset of RRD, retinal pigment epithelium cells lose their epithelial properties and form fibrous membranes on the retinal surface[18]. The pathogenesis of proliferative vitreoretinopathy is closely related to the epithelial-mesenchymal transition in retinal pigment epithelium cells, which is characterized by the downregulation of E-cadherin and the upregulation of N-cadherin. After the epithelial-mesenchymal transition, the expression levels of E-cadherin and keratin were decreased, whereas the expression levels of α-smooth muscle actin (α-SMA) and fibronectin

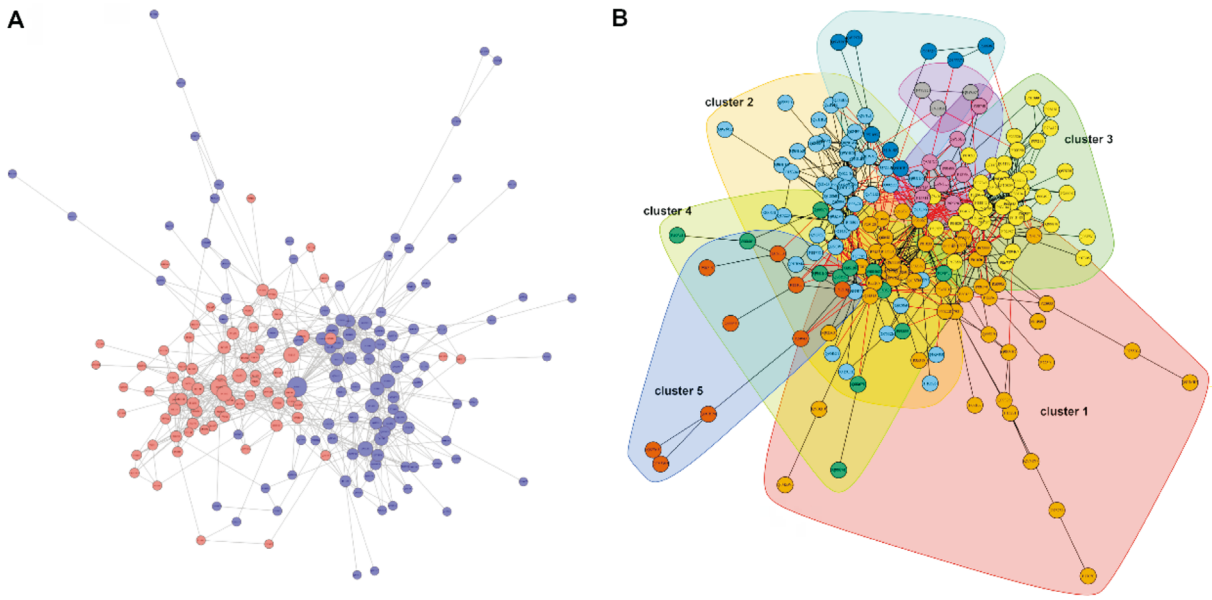

Figure 5 Protein-protein interaction network of DEPs and functional classification diagram A: Red nodes indicate upregulation; blue nodes indicate downregulation. B: Dividing the highly aggregated proteins in the interaction network graph into different clusters. DEPs: Differently expressed proteins.

were increased[19-20]. Elevated expression of E-cadherin is reportedly sufficient to inhibit epithelial-mesenchymal transition and proliferation in retinal pigment epithelium cells; this inhibits transforming growth factor (TGF)-β1-induced apoptosis, thereby delaying RRD progression to proliferative vitreoretinopathy[21]. The above findings are consistent with our results.

In the present study, we found that patients with RRD demonstrated the activation of acute inflammation-related processes in the vitreous; these processes involved neutrophil-tropic adhesion and monocyte-macrophage-induced immune responses. Immunity- and inflammation-related signaling molecules contribute to the pathobiology of various vitreoretinal diseases[22]. The expression levels of pro-inflammatory genes are elevated in patients with RRD; downstream effects include increased cytokine expression and subretinal infiltration by monocytes and macrophages[23-24]. Inflammasome activation in retinal diseases is reportedly protective in some instances; in other instances, it may lead to neuronal cell death[25-26]. The onset of RRD leads to macrophage activation and infiltration[22]. Pro-inflammatory and growth factors are released into the vitreous in patients with RRD[27]. Pro-inflammatory cytokines are significantly upregulated, promoting photoreceptor apoptosis in detached retina[28]. The above findings support our experimental results.

Furthermore, we found that the expression levels of heat shock proteins were upregulated in patients with RRD, which may constitute a protective mechanism. A previous study revealed the upregulation of heat shock proteins in vitreous humor samples from patients with RRD[29].

Finally, this study demonstrated that RRD induces the upregulation of glycolytic responses. Among the DEPs identified in this study, enzymes expressed in RRD were related to carbon metabolism and glycolysis. Glycolytic enzymes are reportedly upregulated in RRD to compensate for the metabolic "stress" state within the retina[30]. Elevated levels of α-enolase and upregulation of glycolysis were observed in extracts from rabbits with retinal detachment[31]. The hypoxia-inducible factor (HIF)-1 signaling pathway and glycolytic metabolism were enriched in human vitreous humor[17]. Other studies have shown that glycolysis, photoreceptor death, and Wnt and mitogen-activated protein kinase (MAPK) signaling are activated during RRD; these pathways promote retinal cell survival. Overall, the above findings are consistent with our results.

This study had some limitations. First, we only recruited nine eligible patients; this small sample size may have led to bias in the analysis. Second, our proteomic analysis was based on vitreous humor samples, rather than the examination of retinal cells or tissues. Therefore, the results may only partially reflect biological changes involving retinal neurons in eyes with RRD. Considering the implications of our results, we are recruiting additional patients and collecting more detailed clinical data to validate our metabolomic findings.

In conclusion, the present study revealed that the proteomic characteristics of vitreous humor in patients with RRD were significantly different from the proteomic characteristics of patients in the control group. Further analysis indicated that differential metabolites were mainly enriched in the cell adhesion molecule metabolic pathway. DEPs were related to heat shock protein content, glycolysis, and acute inflammatory

response. These findings may be useful for identification of novel biomarkers for RRD pathogenesis.

ACKNOWLEDGEMENTS

We thank Ryan Chastain-Gross, Ph.D., from Liwen Bianji (Edanz) (www.liwenbianji.cn/) for editing the English text of a draft of this manuscript.

Conflicts of Interest: Huo QY, None; **Zhu MC,** None; **Yang WC,** None; **Wang YP,** None; **Chen S,** None.

REFERENCES

1 Liao L, Zhu XH. Advances in the treatment of rhegmatogenous retinal detachment. *Int J Ophthalmol* 2019;12(4):660-667.

2 Garneau J, Hébert M, You E, Bourgault S, Caissie M, Tourville É, Dirani A. Anatomical and functional outcomes of retinal detachment associated with nontraumatic giant retinal tears compared to simple rhegmatogenous retinal detachment. *Int J Retina Vitreous* 2022;8(1):65.

3 Foos RY, Wheeler NC. Vitreoretinal juncture. Synchysis senilis and posterior vitreous detachment. *Ophthalmology* 1982;89(12): 1502-1512.

4 Tasman WS. Posterior vitreous detachment and peripheral retinal breaks. *Trans Am Acad Ophthalmol Otolaryngol* 1968;72(2): 217-224.

5 Znaor L, Medic A, Binder S, Vucinovic A, Marin Lovric J, Puljak L. Pars Plana vitrectomy versus scleral buckling for repairing simple rhegmatogenous retinal detachments. *Cochrane Database Syst Rev* 2019;3(3):CD009562.

6 Sodhi A, Leung LS, Do DV, Gower EW, Schein OD, Handa JT. Recent trends in the management of rhegmatogenous retinal detachment. *Surv Ophthalmol* 2008;53(1):50-67.

7 Santos FM, Mesquita J, Castro-de-Sousa JP, Ciordia S, Paradela A, Tomaz CT. Vitreous humor proteome: targeting oxidative stress, inflammation, and neurodegeneration in vitreoretinal diseases. *Antioxidants* (*Basel*) 2022;11(3):505.

8 Pinilla I, Maneu V, Campello L, Fernández-Sánchez L, Martínez-Gil N, Kutsyr O, Sánchez-Sáez X, Sánchez-Castillo C, Lax P, Cuenca N. Inherited retinal dystrophies: role of oxidative stress and inflammation in their physiopathology and therapeutic implications. *Antioxidants* (*Basel*) 2022;11(6):1086.

9 Shu DY, Chaudhary S, Cho KS, Lennikov A, Miller WP, Thorn DC, Yang ML, McKay TB. Role of oxidative stress in ocular diseases: a balancing act. *Metabolites* 2023;13(2):187.

10 Kustatscher G, Collins T, Gingras AC, Guo TN, Hermjakob H, Ideker T, Lilley KS, Lundberg E, Marcotte EM, Ralser M, Rappsilber J. Understudied proteins: opportunities and challenges for functional proteomics. *Nat Methods* 2022;19(7):774-779.

11 Loginov DS, Fiala J, Chmelik J, Brechlin P, Kruppa G, Novak P. Benefits of ion mobility separation and parallel accumulation-serial fragmentation technology on timsTOF pro for the needs of fast photochemical oxidation of protein analysis. *ACS Omega* 2021;6(15):10352-10361.

12 Li J, Pan H, Yang H, Wang C, Liu HH, Zhou H, Li PW, Li CZ, Lu XY, Tian Y. Rhamnolipid enhances the nitrogen fixation activity of *Azotobacter chroococcum* by influencing lysine succinylation. *Front Microbiol* 2021;12:697963.

13 Bhattacharyya IM, Cohen S, Shalabny A, Bashouti M, Akabayov B, Shalev G. Specific and label-free immunosensing of protein-protein interactions with silicon-based immunoFETs. *Biosens Bioelectron* 2019;132:143-161.

14 Kuhn F, Aylward B. Rhegmatogenous retinal detachment: a reappraisal of its pathophysiology and treatment. *Ophthalmic Res* 2014;51(1):15-31.

15 Mervin K, Valter K, Maslim J, Lewis G, Fisher S, Stone J. Limiting photoreceptor death and deconstruction during experimental retinal detachment: the value of oxygen supplementation. *Am J Ophthalmol* 1999;128(2):155-164.

16 Öhman T, Gawriyski L, Miettinen S, Varjosalo M, Loukovaara S. Molecular pathogenesis of rhegmatogenous retinal detachment. *Sci Rep* 2021;11(1):966.

17 Shu YY, Gao M, Zhou YF, Liu HY, Sun XD. DIA comparative proteomic analysis of retro-oil fluid and vitreous fluid from retinal detachment patients. *Front Mol Biosci* 2021;8:763002.

18 Ishikawa K, Akiyama M, Mori K, Nakama T, Notomi S, Nakao S, Kohno RI, Takeda A, Sonoda KH. Drainage retinotomy confers risk of epiretinal membrane formation after vitrectomy for rhegmatogenous retinal detachment repair. *Am J Ophthalmol* 2022;234:20-27.

19 Jin HZ, Cai WT, Yu DH, Fan JQ, Liu QY, Yu J. Development of proliferative vitreoretinopathy is attenuated by chicken ovalbumin upstream promoter transcriptional factor 1 via inhibiting epithelial-mesenchymal transition. *Discov Med* 2022;34(172):103-113.

20 Yang HY, Bai Y, Fu C, Liu WH, Diao ZL. Exosomes from high glucose-treated macrophages promote epithelial-mesenchymal transition of renal tubular epithelial cells via long non-coding RNAs. *BMC Nephrol* 2023;24(1):24.

21 Wei JY, Wu LJ, Yang S, Zhang CH, Feng L, Wang ML, Li H, Wang F. E-cadherin to N-cadherin switching in the TGF-β1 mediated retinal pigment epithelial to mesenchymal transition. *Exp Eye Res* 2022;220:109085.

22 Sene A, Apte RS. Inflammation-induced photoreceptor cell death. *Adv Exp Med Biol* 2018;1074:203-208.

23 Lewandowska-Furmanik M, Pozarowska D, Pozarowski P, Matysik A. TH1/TH2 balance in the subretinal fluid of patients with rhegmatogenous retinal detachment. *Med Sci Monit* 2002;8(7): CR526-CR528.

24 Kiang L, Ross BX, Yao JY, Shanmugam S, Andrews CA, Hansen SA, Besirli CG, Zacks DN, Abcouwer SF. Vitreous cytokine expression and a murine model suggest a key role of microglia in the inflammatory response to retinal detachment. *Invest Ophthalmol Vis Sci* 2018;59(8):3767-3778.

25 Mugisho OO, Green CR. The NLRP3 inflammasome in age-related eye disease: evidence-based connexin hemichannel therapeutics. *Exp Eye Res* 2022;215:108911.

26 Déchelle-Marquet PA, Guillonneau X, Sennlaub F, Delarasse C. P2X7-dependent immune pathways in retinal diseases. *Neuropharmacology* 2023;223:109332.

27 Ananikas K, Stavrakas P, Kroupis C, Christou EE, Brouzas D, Petrou P, Papakonstantinou D. Molecular biologic milieu in rhegmatogenous retinal detachment and proliferative vitreoretinopathy: a literature review. *Ophthalmic Res* 2022;65(6):637-646.

28 Matsumoto H, Sugio S, Seghers F, Krizaj D, Akiyama H, Ishizaki Y, Gailly P, Shibasaki K. Retinal detachment-induced Müller glial cell swelling activates TRPV4 ion channels and triggers photoreceptor death at body temperature. *J Neurosci* 2018;38(41):8745-8758.

29 Santos FM, Gaspar LM, Ciordia S, Rocha AS, Castro E Sousa JP, Paradela A, Passarinha LA, Tomaz CT. iTRAQ quantitative proteomic analysis of vitreous from patients with retinal detachment. *Int J Mol Sci* 2018;19(4):1157.

30 She XJ, Zhou YF, Liang Z, *et al*. Metabolomic study of a rat model of retinal detachment. *Metabolites* 2022;12(11):1077.

31 Tamhane M, Cabrera-Ghayouri S, Abelian G, Viswanath V. Review of biomarkers in ocular matrices: challenges and opportunities. *Pharm Res* 2019;36(3):40.